

LETTER TO THE EDITOR

# 3HSP J095507.9+355101: a flaring extreme blazar coincident in space and time with IceCube-200107A

P. Giommi<sup>1,2,3</sup>, P. Padovani<sup>4,5</sup>, F. Oikonomou<sup>4,6,7</sup>, T. Glauch<sup>1,6</sup>, S. Paiano<sup>8,9</sup>, and E. Resconi<sup>6</sup>

<sup>1</sup> Institute for Advanced Study, Technische Universität München, Lichtenbergstrasse 2a, D-85748 Garching bei München, Germany

<sup>2</sup> Associated to Agenzia Spaziale Italiana, ASI, via del Politecnico s.n.c., I-00133 Roma, Italy

<sup>3</sup> ICRA Net, Piazzale della Repubblica 10, I-65122, Pescara, Italy

<sup>4</sup> European Southern Observatory, Karl-Schwarzschild-Str. 2, D-85748 Garching bei München, Germany

<sup>5</sup> Associated to INAF - Osservatorio Astronomico di Roma, via Frascati 33, I-00040 Monteporzio Catone, Italy

<sup>6</sup> Technische Universität München, Physik-Department, James-Frank-Str. 1, D-85748 Garching bei München, Germany

<sup>7</sup> Institutt for fysikk, NTNU, Trondheim, Norway

<sup>8</sup> INAF - Osservatorio Astronomico di Roma, via Frascati 33, I-00040, Monteporzio Catone, Italy

<sup>9</sup> INAF - IASF Milano, via Corti 12, I-20133, Milano, Italy

e-mail: giommipaolo@gmail.com

June 28, 2022

## ABSTRACT

The uncertainty region of the highly energetic neutrino IceCube200107A includes 3HSP J095507.9+355101 ( $z = 0.557$ ), an extreme blazar, which was detected in a high, very hard and variable X-ray state shortly after the neutrino arrival. Following a detailed multi-wavelength investigation, we confirm that the source is a genuine BL Lac, contrary to TXS 0506+056, the first source so far associated with IceCube neutrinos, which is a “masquerading” BL Lac. As in the case of TXS 0506+056, 3HSP J095507.9+355101 is also way off the so-called “blazar sequence”. We consider 3HSP J095507.9+355101 a possible counterpart to the IceCube neutrino. Finally, we discuss some theoretical implications in terms of neutrino production.

**Key words.** neutrinos — radiation mechanisms: non-thermal — galaxies: active — BL Lacertae objects: general — gamma-rays: galaxies

## 1. Introduction

The IceCube Neutrino Observatory at the South Pole<sup>1</sup> has detected tens of high-energy neutrinos of likely astrophysical origin (e.g. [IceCube Collaboration 2017b](#); [Schneider 2020](#); [Stettner 2020](#), and references therein). So far, only one astronomical object has been significantly associated (in space and time) with some of these neutrinos, i.e. the bright blazar TXS 0506+056 at  $z = 0.3365$  ([IceCube Collaboration et al. 2018](#); [IceCube Collaboration 2018](#); [Padovani et al. 2018](#); [Paiano et al. 2018](#)). The case for blazars being neutrino sources, however, is mounting. Several studies have reported hints of a correlation between blazars and the arrival direction of astrophysical neutrinos (e.g. [Padovani & Resconi 2014](#); [Padovani et al. 2016](#); [Lucarelli et al. 2019](#) and references therein; but see also [IceCube Collaboration 2017a](#)) and possibly of Ultra High Energy Cosmic Rays ([Resconi et al. 2017](#)). Moreover, very recently some of us ([Giommi et al. 2020a](#)) have extended the detailed dissection of the region around the IceCube-170922A event related to TXS 0506+056 carried out by [Padovani et al. \(2018\)](#) to all the 70 public IceCube high-energy neutrinos that are well reconstructed (so-called tracks) and off the Galactic plane. This resulted in a  $3.23\sigma$  (post-trial) excess of IBLs<sup>2</sup> and HBLs with a best-fit of  $15 \pm 4$  signal sources, while

no excess was found for LBLs. Given that TXS 0506+056 is also a blazar of the IBL/HBL type ([Padovani et al. 2019](#)) this result, together with previous findings, consistently points to growing evidence for a connection between IceCube neutrinos and IBL and HBL blazars. We report here on 3HSP J095507.9+355101, an HBL within the error region of the IceCube track IceCube-200107A (see Fig. 1), which was found to exhibit an X-ray flare the day after the neutrino arrival. This source belongs to the third high-synchrotron peaked (3HSP) catalogue ([Chang et al. 2019](#)), which includes blazars with  $\nu_{\text{peak}}^S > 10^{15}$  Hz. Actually, with a catalogued synchrotron peak frequency of  $\sim 5 \times 10^{17}$  Hz, and a significantly higher value during the flare (Sec. 2.2), this source belongs to the rare class of extreme blazars (e.g. [Biteau et al. 2020](#), and references therein). We also comment on the nature of the source and on the theoretical implications in terms of neutrino production. We use a  $\Lambda$ CDM cosmology with  $H_0 = 70$  km  $\text{s}^{-1}$   $\text{Mpc}^{-1}$ ,  $\Omega_{\text{m},0} = 0.3$ , and  $\Omega_{\Lambda,0} = 0.7$ .

## 2. Multi-messenger data

### 2.1. IceCube data

On January 7, 2020 the IceCube Collaboration reported the detection of a high-energy neutrino candidate (HESE, [Stein 2020](#)) of possible astrophysical origin. While the event was not selected and high-energy ( $\nu_{\text{peak}}^S > 10^{15}$  Hz [ $> 4.1$  eV]) peaked (IBL and HBL) sources respectively ([Padovani & Giommi 1995](#); [Abdo et al. 2010](#)).

<sup>1</sup> <http://icecube.wisc.edu>

<sup>2</sup> Blazars are divided based on the rest-frame frequency of the low-energy (synchrotron) hump ( $\nu_{\text{peak}}^S$ ) into LBL sources ( $\nu_{\text{peak}}^S < 10^{14}$  Hz [ $< 0.41$  eV]), intermediate- ( $10^{14}$  Hz  $< \nu_{\text{peak}}^S < 10^{15}$  Hz [ $0.41$  eV –  $4.1$  eV]),

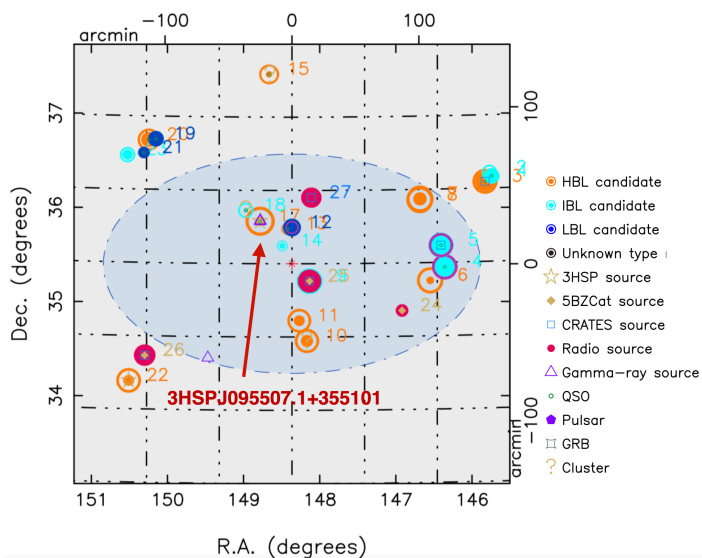


**Fig. 1.** Known and candidate blazars (radio/X-ray matching sources) around the 90% containment region of IceCube200107A, approximated by the darker elliptical area.

by the standard real-time detection procedure, it was identified as a starting track by a newly developed deep neural-network event classifier (Kronmueller & Glauch 2020). After applying off-line reconstructions the arrival direction is given as right ascension  $148.18^{+2.20}_{-1.83}$  deg and declination  $35.46^{+1.10}_{-1.22}$  deg at 90% C.L. As this was an unscheduled report, IceCube does not provide any energy information. Assuming an  $E^{-2}$  ( $E^{-1}/E^{-2.7}$ ) spectrum and the effective area for HESF starting tracks (IceCube Collaboration 2014) we find, however, an average expected energy of  $\sim 334$  TeV (1.4 PeV/156 TeV) respectively. Further hints for the event being astrophysical comes from the direction. Being clearly up-going, an atmospheric muon origin can be excluded. Also the fraction of the conventional atmospheric muon neutrino background is suppressed compared to the horizon. In a follow-up GCN report (Pizzuto 2020) IceCube announced the detection of two additional neutrino candidates in spatial coincidence with the 90% containment region of IceCube-200107A in a time range of two days around the alert and consistent with atmospheric background at a 4% level. Note that the error region of IceCube-200107A is also fully inside the  $16.5^\circ$  median angular error circle of a HESF shower detected by IceCube in 2011 (HES9), and reported in IceCube Collaboration (2014). In fact 3HSP J095507.9+355101 is located only  $0.62^\circ$  and  $2.73^\circ$  away from the best-fit position of IceCube-200107A and HES9, respectively.

We estimate the flux required to detect, on average, one muon neutrino with IceCube at a specified time interval,  $\Delta T$  by assuming the neutrino event, IceCube-200107A, to be a signal event. The number of signal-only, muon (and antimuon) neutrinos detected during  $\Delta T$  at declination  $\delta$  is given by  $N_{\nu_\mu} = \int_{E_{\nu_\mu, \min}}^{E_{\nu_\mu, \max}} dE_{\nu_\mu} A_{\text{eff}}(E_{\nu_\mu}, \delta) \phi_{E_{\nu_\mu}} \Delta T$ , where  $E_{\nu_\mu, \min}$  and  $E_{\nu_\mu, \max}$  are the 90% C.L. lower and upper limits on the energy of the neutrino respectively,  $A_{\text{eff}}$  is the effective area, and  $\phi_{E_{\nu_\mu}}$  the muon neutrino flux differential in energy. We assume a source emitting an  $E^{-2}$  neutrino spectrum between 65 TeV and 2.6 PeV, the 90% containment range for the energy of IC-200107A. Since the neutrino emission duration is unknown we calculate the neutrino flux for  $\Delta T = 30$  d/250 d/10 yr, corresponding to the lower limit on the duration of the UV/soft X-ray flare (Sec. 2.2), the *Fermi* integration time (Sec. 2.4) and the dura-

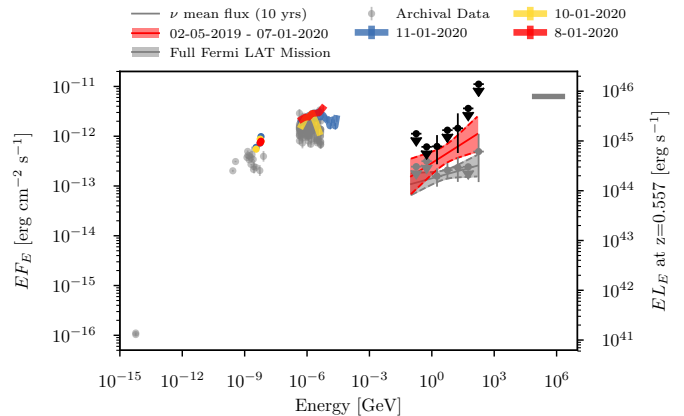


**Fig. 2.** The SED of 3HSP J095507.1+355101: grey points refer to archival data and, in the case of *Fermi*-LAT data, the time-integrated measurement up to the arrival of the neutrino alert. The mean all-flavour neutrino flux is shown for an assumed live time of 10 yr. Coloured data-points are Swift and NuSTAR measurements made around the neutrino arrival time. The black  $\gamma$ -ray points refer to the red bow-tie.

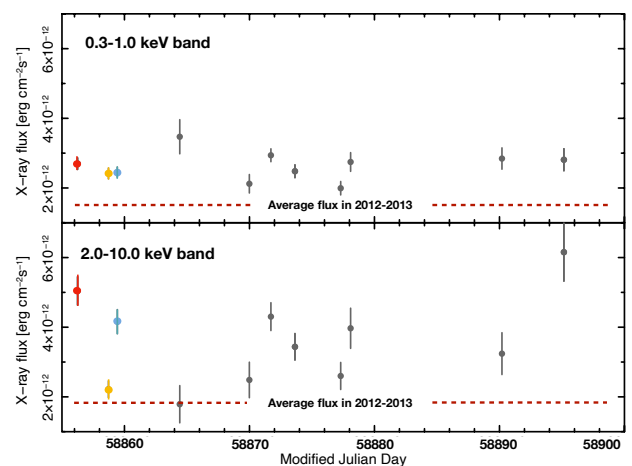


**Fig. 3.** Swift Soft and hard X-ray monitoring of 3HSPJ095507.1+355101 after the neutrino arrival. The first observation was carried out one day after the detection of IC200107A. Colours match the ones used in the SED of Fig. 2. Note that the flux is higher than the average observed in 2012-2013 in both bands, but short-term variability is only present in the 2 – 10 KeV energy band.

tion of the IceCube operation respectively. Using the effective area of Blaufuss et al. (2020) we obtain an integrated, all-flavour neutrino energy flux, in the 90% containment energy range, of  $3 \times 10^{-9}/4 \times 10^{-10}/3 \times 10^{-11}$  erg cm $^{-2}$  s $^{-1}$  respectively, corresponding to an average, integrated all-flavour neutrino luminosity of  $\mathcal{L}_\nu \approx 4 \times 10^{48}/5 \times 10^{47}/3 \times 10^{46}$  erg s $^{-1}$ . For a population of neutrino producing sources with summed expectation of order one neutrino, the energy flux estimate given above roughly corresponds to the total energy flux produced by the source population, whereas the individual source contribution, and thus the individual neutrino luminosity is much lower than our estimate above (IceCube Collaboration et al. 2018).

## 2.2. Swift data

The *Neil Gehrels Swift* observatory (Gehrels et al. 2004) observed 3HSP J095507.9+355101 37 times; 26 pointings were

performed between 2012 and 2013, and the remaining ones have been carried out either as a Target of Opportunity (ToO), after the IceCube200107A event, which revealed the source to be in a flaring and very hard state (Giommi et al. 2020b; Krauss et al. 2020) and as part of a subsequent monitoring program. We analysed all the X-Ray Telescope (XRT; Burrows et al. 2005) imaging data using *Swift-DeepSky*, a Docker container<sup>3</sup> encapsulated pipeline software developed in the context of the Open Universe initiative (Giommi et al. 2018, 2019). Spectral analysis was also performed on all exposures with sufficiently strong signal using the XSPEC-12 software embedded in a dedicated processing pipeline, called *Swift-xrtproc*, first presented in Giommi (2015). The 2 – 10 keV emission from 3HSP J095507.9+355101 exhibited over a factor of ten variability in intensity associated with strong spectral changes following a harder-when-brighter trend. The ToO observation of 3HSP J095507.9+355101 found this object in a flaring and hard state, with a 2 – 10 keV X-ray flux of  $\sim 5 \times 10^{-12}$  erg cm<sup>-2</sup> s<sup>-1</sup> a factor 2.5 larger than the average value observed in 2012 – 2013, and with a power law spectral index  $\Gamma = 1.8 \pm 0.06$ . A log-parabola model gives a similar slope at 1 keV and curvature parameter consistent with zero, implying  $\nu_{\text{peak}}^S \gtrsim 2 \times 10^{18}$  Hz. The optical and UV data of the Ultra-Violet and Optical telescope (UVOT; Roming et al. 2005) were analyzed using the on-line tools of the SSDC interactive archive<sup>4</sup>. Spectral data are shown in Fig. 2, while the X-ray light-curve is shown in Fig. 3. The optical/UV and low energy X-ray data reach their maximum intensity after the neutrino arrival and remain approximately constant for the subsequent  $\sim 30$  days, implying that all the variability in the 2 – 10 keV band is induced by strong spectral changes above  $\sim 7.3 \times 10^{17}$  Hz.

### 2.3. NuSTAR data

3HSP J095507.9+355101 was observed by the *NuSTAR* hard X-ray observatory (Harrison et al. 2013) four days after the detection of IceCube-200107A, following the results of the *Swift* ToO mentioned above. The observation was partly simultaneous with the third *Swift* observation after the neutrino event. We have analysed the data, which were made openly available, using the online analysis tools of the SSDC multi-mission archive, following the standard procedure. The source was detected between 3 and  $\sim 30$  keV. A power law spectral fit gives a best fit slope of  $\Gamma = 2.21 \pm 0.06$  with a reduced  $\chi^2_{\nu} = 0.94$ . The data, converted to SED units, are shown as light blue symbols in Fig. 2.

### 2.4. Fermi-LAT data

For the analysis of the  $\gamma$ -ray emission of 3HSP J095507.9+355101 we used the publicly available Fermi-LAT Pass 8 data acquired in the period August 4, 2008 to January 8, 2020 and followed the standard procedure as described in the *Fermi* cicerone<sup>5</sup>. We constructed a model that contains all known 4FGL sources plus the diffuse Galactic and isotropic emissions. In the likelihood fits the normalization and spectral index of all sources within  $10^\circ$  (corresponding to the 95% *Fermi* point-spread function at 100 MeV) are left free. To calculate an a priori estimate of the required integration time for a significant detection of the source, we used the time-integrated measurement in the *Fermi* 4FGL catalogue.

Assuming a signal dominated counting experiment with  $\chi^2_1$  background test-statistic distribution we know that the median test statistic distribution scales linearly in time  $t$ , i.e.  $\mathcal{TS} \propto t$  and therefore

$$t_{lc} = (\mathcal{TS}_{lc} / \mathcal{TS}_{2920d}) \cdot 2920 \text{ [days]} \quad (1)$$

assuming a quasi-steady emission. Here  $\mathcal{TS}_{lc}$  defines the target test-statistic value with required integration time  $t_{lc}$ . 2920 days and  $\mathcal{TS}_{2920d}$  are the live time and significance of the source in the 4FGL catalogue, respectively. Note that in general for the significance  $\Sigma = \sqrt{\mathcal{TS}}$ . The source is detected with a significance of  $5.42\sigma$  in the 4FGL catalogue and hence the resulting integration times for one and two sigma are 100 and 400 days, respectively. In order to avoid washing out a possible time-dependent signal we chose an integration time of 250 days. The resulting fit between MJD 58605.6 and 58855.6 gives a detection with a significance of  $2.9\sigma$  and spectral index  $\Gamma = 1.73 \pm 0.31$  for a typical single power-law model. The spectral index over the full-mission is  $\Gamma = 1.88 \pm 0.15$ , with photon associations up to 178 GeV at 99 % C.L. The corresponding photon fluxes integrated over the entire energy range are  $1.33 \times 10^{-9}$  ph cm<sup>-2</sup> s<sup>-1</sup> and  $7.7 \times 10^{-10}$  ph cm<sup>-2</sup> s<sup>-1</sup>, respectively. The fit results are also visualized in Figure 2.

### 2.5. LBT data

3HSP J095507.9+355101 was observed on January 29, 2020 at the Large Binocular Telescope (LBT; Pogge et al. 2010) in the optical band (4, 100 – 8, 500 Å). A firm redshift  $z = 0.557$  was derived thanks to the clear detection of absorption features attributed to its host galaxy. No narrow emission line was detected down to an equivalent width  $\sim 0.3$  Å. This corresponds to [O II] and [O III] line luminosities  $< 2 \times 10^{40}$  erg s<sup>-1</sup>. Details about the spectroscopic study of the source, its host galaxy, and close environment are given in Paiano et al. (2020).

## 3. The nature of 3HSP J095507.9+355101

The SED of 3HSP J095507.9+355101, assembled using multi-frequency historical data, shows that this source exhibits a  $\nu_{\text{peak}}^S \sim 5 \times 10^{17}$  Hz (Chang et al. 2019), a very large value that is rarely reached even by extreme blazars (Biteau et al. 2020). The 3HSP catalogue includes only 80 sources with  $\nu_{\text{peak}}^S \geq 5 \times 10^{17}$  Hz that have been detected by Fermi-LAT in  $\sim 34,000$  square degrees of high Galactic latitude sky ( $|b| > 10^\circ$ ), corresponding to an average density of one object every 425 square degrees. The chance probability that one such extreme source is included in the 7.3 square degrees error region of IC200107A is therefore 7.3/425, or about 1.7%. At the time of the neutrino detection 3HSP J095507.9+355101 was also found to be in a very hard state ( $\nu_{\text{peak}}^S \gtrsim 2 \times 10^{18}$  Hz [10 keV] and flaring; see Fig. 2). We used the Open Universe blazar database to estimate how frequently extreme sources of this type (e.g. MRK421, MRK501 etc.), and observed by Swift more than a hundred times, are found in a flare state, finding that they spend less than 10% of the time at an intensity that is larger than twice the average value. The overall chance probability of finding a blazar with  $\nu_{\text{peak}}^S$  as high as that of 3HSP J095507.9+355101 in the error region of IceCube-200107A during a flaring event is therefore a fraction of 1%. Since this is a posterior estimation based on archival data, which may hide possible biases, it should not be taken as evidence for a firm association, but rather as the identification

<sup>3</sup> <https://www.docker.com>

<sup>4</sup> <http://www.ssdsc.asi.it>

<sup>5</sup> <https://fermi.gsfc.nasa.gov/ssc/data/analysis/documentation/Cicerone/>

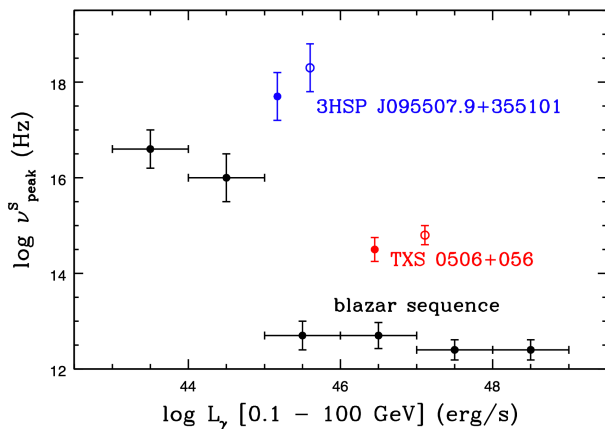


**Fig. 4.**  $\nu_{\text{peak}}^S$  versus  $L_\gamma$  for the revised blazar sequence (black points; Ghisellini et al. 2017) and TXS 0506+056 and 3HSP J095507.9+355101 (red and blue points respectively: average [filled] and  $\gamma$ -ray flare [open] values). The TXS 0506+056 values are from Padovani et al. (2019). The error bars denote the sample dispersion (blazar sequence) and the uncertainty (TXS 0506+056 and 3HSP J095507.9+355101) respectively.

of an uncommon and physically interesting event that corroborates a persistent trend (e.g. IceCube Collaboration et al. 2018; Giommi et al. 2020a) and motivates this work. We have studied the nature of 3HSP J095507.1+355101, following Padovani et al. (2019), to check if this source is also a “masquerading” BL Lac like TXS 0506+056, i.e., intrinsically a flat-spectrum radio quasar (FSRQ) with the emission lines heavily diluted by a strong, Doppler-boosted jet. Given the upper limits on its  $L_{O\text{II}}$  and  $L_{O\text{III}}$  and its black hole mass estimate ( $M_{\text{BH}} \sim 3 \times 10^8 M_\odot$ ; Paiano et al. 2020), we obtain the following results: 1. its radio and  $O\text{II}$  luminosities put it at the very edge of the locus of jetted quasars (Fig. 4 of Kafoutzou et al. 2012); 2. its Eddington ratio is  $L/L_{\text{Edd}} < 0.02$ , formally still within the range of high-excitation galaxies (HEGs, characterized by  $L/L_{\text{Edd}} \gtrsim 0.01$ ) but barely so; 3. its broad-line region (BLR) power in Eddington units is  $L_{\text{BLR}}/L_{\text{Edd}} < 3 \times 10^{-4}$ , which implies that this source is not an FSRQ according to Ghisellini et al. (2011) (as this would require  $L_{\text{BLR}}/L_{\text{Edd}} \gtrsim 5 \times 10^{-4}$ ); 4. finally, its  $L_\gamma/L_{\text{Edd}}$  values range between  $\sim 0.04$  and  $\sim 0.10$ , depending on its state, i.e. they straddle the BL Lac – FSRQ division proposed by Sbarrato et al. (2012) ( $L_\gamma/L_{\text{Edd}} \sim 0.1$ ). Based on all of the above we consider 3HSP J095507.1+355101 an unlikely “masquerading” BL Lac. Fig. 4 shows the location of 3HSP J095507.1+355101 on the  $\nu_{\text{peak}}^S$  versus  $L_\gamma$  plane in its average state (blue filled point) and during the flare (blue open point). The source is an extreme outlier of the so-called blazar sequence, even more so than TXS 0506+056. Given its  $L_\gamma$ , in fact, its  $\nu_{\text{peak}}^S$  should be about five orders of magnitude smaller to fit the sequence.

#### 4. Theoretical considerations and conclusion

We now make some brief theoretical considerations based on multi-wavelength observations of 3HSP J095507.9+355101. A more complete treatment is given in Petropoulou et al. 2020 (in preparation). Neutrino production in the blazar jet is most likely facilitated by photopion ( $p\pi$ ) interactions, characterised by the optical depth  $f_{p\pi}$ . Of the energy lost by protons with energy  $\varepsilon_p$  in  $p\pi$  interactions, 3/8ths go to neutrinos, resulting in the production of neutrinos with all-flavour luminosity,

$\varepsilon_\nu L_{\varepsilon_\nu} = (3/8)f_{p\pi}\varepsilon_p L_{\varepsilon_p}$ . Each neutrino is produced with energy  $\varepsilon_\nu \approx 0.05\varepsilon_p$ . Here and throughout,  $\varepsilon L_\varepsilon$  is the luminosity per logarithmic energy,  $\varepsilon \cdot dL/d\varepsilon$ , unprimed symbols denote quantities in the cosmic rest frame, quantities with the subscript “obs” refer to the observer frame, and primed quantities refer to the frame comoving with the jet. Neutrinos produced in interactions with photons comoving with the jet have typical energy  $\varepsilon_{\nu,\text{obs}} \approx 7.5 \text{ PeV} (\varepsilon_t/2 \text{ keV})^{-1} (\Gamma/20)^2 (1+z)^{-2}$ , where  $\Gamma$  is the bulk Lorentz factor of the jet, and  $\varepsilon_t$  the energy of the target photons assuming that protons are accelerated to at least 150 PeV.

The remaining 5/8ths of the proton energy lost go towards the production of electrons and pionic  $\gamma$ -rays. Synchrotron emission from electrons/positrons produced in  $p\pi$  interactions and two-photon annihilation of the pionic  $\gamma$ -rays result in synchrotron cascade flux (Murase et al. 2018)

$$\varepsilon_\nu L_{\varepsilon_\nu} \approx \frac{6(1+Y_{\text{IC}})}{5} \varepsilon_\gamma L_{\varepsilon_\gamma} \Big|_{\varepsilon_{\text{syn}}^{\text{p}\pi}} \approx 8 \times 10^{44} \text{ erg s}^{-1} \left( \frac{\varepsilon_\gamma L_{\varepsilon_\gamma} \Big|_{\varepsilon_{\text{syn}}^{\text{p}\pi}}}{7 \times 10^{44}} \right) \quad (2)$$

where  $Y_{\text{IC}}$  is the Compton-Y parameter, typically expected to be  $Y_{\text{IC}} \ll 1$  and the  $\gamma$ -ray emission is expected at energy  $\varepsilon_{\text{syn}}^{\text{p}\pi} \approx 39.4 \text{ GeV} (B/10^{-0.5} \text{ G})(\varepsilon_{\nu,\text{obs}}/7.5 \text{ PeV})^2 (20/\delta)(1+z)^{-1}$ . The 250-day average luminosity of the flaring SED of 3HSP J095507.9+355101 in the *Fermi*-LAT energy range thus imposes a limit to the average neutrino luminosity according to Eq. 2. If the neutrino emission lasted 250 days, the expected neutrino luminosity of Eq. 2, is  $\sim 2.2$  orders of magnitude lower than the flux implied by the detection of one neutrino according to the estimate of Sec. 2.1, which is  $\varepsilon_\nu L_{\varepsilon_\nu} = \mathcal{L}_\nu / \ln(2.6 \text{ PeV}/65 \text{ TeV}) \approx 1.3 \times 10^{47} \text{ erg s}^{-1}$ . The expected neutrino luminosity as a function of the proton luminosity is shown in Fig. 5, for two characteristic values of  $f_{p\pi}$  (by definition  $f_{p\pi} \leq 1$ ), together with the constraint imposed by Eq. 2 and the luminosity needed to produce 1 neutrino in IceCube. Fig. 5 also gives the “baryon loading” factor,  $\xi$ , implied by a given proton luminosity, defined here as  $\xi = \varepsilon_p L_{\varepsilon_p} / \varepsilon_\nu L_{\varepsilon_\nu}$ . Considering the long-term average *Fermi*-LAT flux instead, Eq. 2 leads to an upper limit on  $\varepsilon_\nu L_{\varepsilon_\nu} \approx [6/(1+Y_{\text{IC}})] \varepsilon_\gamma L_{\varepsilon_\gamma} \Big|_{\varepsilon_{\text{syn}}^{\text{p}\pi}} \approx 3 \times 10^{44} \text{ erg s}^{-1}$ . This is a factor of  $\sim 30$  lower than the neutrino luminosity needed to detect 1 neutrino in IceCube, assuming a 10-yr lifetime, which is  $\mathcal{L}_\nu / \ln(2.6 \text{ PeV}/65 \text{ TeV}) \approx 8 \times 10^{45} \text{ erg s}^{-1}$ . Thus, if the neutrino emission was related to the long-term emission of 3HSP J095507.9+355101, it is easier to satisfy the  $\gamma$ -ray emission constraint than if the neutrino emission was related to the *Fermi*-LAT 250 day high-state. These results are also summarised in Fig. 5. Below the threshold for  $p\pi$  interactions, protons lose energy via the Bethe-Heitler (BH) process. Unlike in the case of TXS 0506+056 for 3HSP J095507.9+355101 there are no observations available to constrain the BH cascade component and the most stringent constraint on the neutrino luminosity comes from the  $p\pi$  cascade.

Fig. 5, reveals the difficulty of canonical theoretical models to explain the observation of one neutrino from 3HSP J095507.9+355101 during the 250 d *Fermi* high state, and to a lesser extent during the 10 yr of IceCube observations. The Poisson probability to detect one neutrino is  $\sim 0.01$  and  $\sim 0.03$  for the two timescales respectively, which could be interpreted as a statistical fluctuation to account for the association. Note, that a similar neutrino luminosity upper limit has been derived in one-zone models of neutrino production of TXS 0506+056 during

<sup>6</sup> We have approximated  $\varepsilon_\nu L_{\varepsilon_\nu} \sim \mathcal{L}_\nu / \ln(320 \text{ GeV}/100 \text{ MeV})$ , where  $\mathcal{L}_\nu = 5.66 \times 10^{45} \text{ erg s}^{-1}$  is the  $\gamma$ -ray luminosity measured with the *Fermi*-LAT during the 250-day flare.

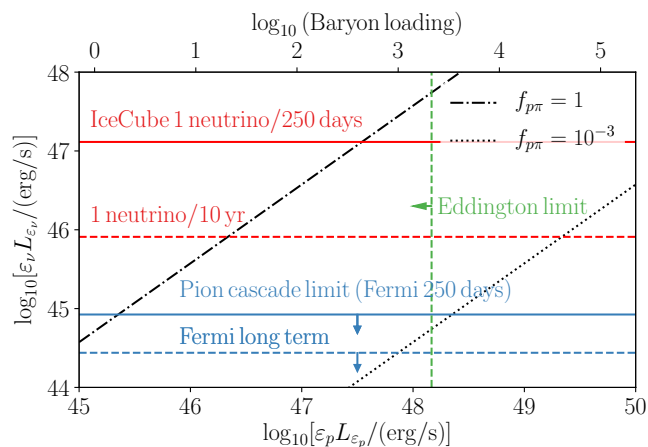


**Fig. 5.** All-flavour neutrino luminosity as a function of proton luminosity for two different values of the optical depth to photopion interactions  $f_{p\pi}$ . The red solid (dashed) line gives the neutrino luminosity corresponding to 1 muon neutrino in IceCube from 3HSP J095507.9+355101 if the neutrino emission lasted 250 days (10 yr). The blue horizontal solid (dashed) line gives the upper limit to the neutrino luminosity implied by the *Fermi*-LAT 250-day (long-term average) spectrum. The green line shows the upper limit to the proton luminosity implied by the Eddington luminosity of the  $3 \times 10^8 M_\odot$  black hole, assuming  $\Gamma = 20$ , proton spectral index  $-2$ , and maximum proton energy  $10^{18}$  eV.

its 2017 flare (Ansoldi et al. 2018; Cerruti et al. 2019; Gao et al. 2019; Keivani et al. 2018; Petropoulou et al. 2020), which must also be interpreted as an upward ( $\sim 2\sigma$ ) fluctuation to account for the observed association. On the other hand, Eq. 2 assumes that neutrinos and  $\gamma$ -rays are co-spatially emitted. In the presence of multiple emitting zones, and/or an obscuring medium for the  $\gamma$ -rays, the constraint of Eq. 2 can be relaxed and larger neutrino luminosity may be produced by 3HSP J095507.9+355101 (see for example such models for the 2017 flare of TXS 0506+056: Murase et al. 2018; Liu et al. 2019; Oikonomou et al. 2019; Xue et al. 2019; Zhang et al. 2020).

In summary, the Eddington ratio and upper limit to the BLR power we obtained make 3HSP J095507.9+355101 an unlikely “masquerading” BL Lac, while its extremely high  $\nu_{\text{peak}}^S$  and spectacular X-ray flare corroborate a persistent trend of association of high-energy neutrinos with IBLs/HSPs and sources off the blazar sequence. Unlike TXS 0506+056, 3HSP J095507.9+355101 points to a different class of possible neutrino emitting BL Lac objects, which do not possess a (hidden) powerful BLR but with abundant  $> \text{keV}$  photons, owing to the high  $\nu_{\text{peak}}^S$ , which can facilitate PeV neutrino production. As was the case with TXS 0506+056, a possible association points to non-standard (“one-zone”) theoretical models, and/or the existence of an underlying population of sources each expected to produce  $\ll 1$  neutrinos in IceCube but with summed expectation  $\geq 1$ . Fig. 5 reveals that  $\sim 150$  (30) sources identical to 3HSP J095507.9+355101 are needed to produce one neutrino in 250 days (10 years), corresponding to an expectation of  $\lesssim 0.01$  neutrinos from a single blazar of this type. This would imply that the IceCube sensitivity is still below the expected fluxes from similar individual blazars, and the currently observed neutrino counting, if due to blazars, must be driven by large statistical fluctuations. A possible way to reconcile observations with expectations is to consider that there are about 100 catalogued blazars with properties similar to 3HSP J095507.1+355101. If each of these objects emits an average flux of  $\sim 0.01$  neutrinos in

the period considered, we would be in a situation of extremely low counting statistics where the probability of observing one neutrino from a specific blazar is of the order of 1%. Collectively, however, one neutrino would be expected on similar time-scales from one of the  $\sim 100$  randomly distributed blazars in the underlying population. This scenario is consistent with the current situation where only single neutrino events from each candidate counterparts are observed. Examples supporting this view are the extreme blazars 3HSPJ023248.6+201717, 3HSPJ144656.8-265658, and 3HSPJ094620.2+010452, located inside the 90% uncertainty region of IC111216A, IC170506A and IC190819A.

*Acknowledgements.* We acknowledge the use of data and software facilities from the ASI-SSDC and the tools developed within the United Nations “Open Universe” initiative. This work is supported by the Deutsche Forschungsgemeinschaft through grant SFB 1258 “Neutrinos and Dark Matter in Astro and Particle Physics”. We thank Riccardo Middei for his help with the analysis of NuSTAR data. We thank Matthias Huber and Michael Unger for useful discussions on the interpretation of the IceCube observations.

## References

- Abdo, A. A., Ackermann, M., Agudo, I., et al. 2010, *ApJ*, 716, 30  
 Ansoldi, S., Antonelli, L. A., Arcaro, C., et al. 2018, *ApJ*, 863, L10  
 Biteau, J., Prandini, E., Costamante, L., et al. 2020, *Nature Astronomy*, 4, 124  
 Blaufuss, E., Kintscher, T., Lu, L., & Tung, C. F. 2020, *PoS, ICRC2019*, 1021  
 Burrows, D. N., Hill, J. E., Nousek, J. A., et al. 2005, *Space Sci. Rev.*, 120, 165  
 Cerruti, M., Zech, A., Boisson, C., et al. 2019, *MNRAS*, 483, L12  
 Chang, Y. L., Arsioli, B., Giommi, P., Padovani, P., & Brandt, C. H. 2019, *A&A*, 632, A77  
 Gao, S., Fedynitch, A., Winter, W., & Pohl, M. 2019, *Nature Astronomy*, 3, 88  
 Gehrels, N., Chincarini, G., Giommi, P., et al. 2004, *ApJ*, 611, 1005  
 Ghisellini, G., Righi, C., Costamante, L., & Tavecchio, F. 2017, *MNRAS*, 469, 255  
 Ghisellini, G., Tavecchio, F., Foschini, L., & Ghirland a, G. 2011, *MNRAS*, 414, 2674  
 Giommi, P. 2015, *Journal of High Energy Astrophysics*, 7, 173  
 Giommi, P., Arrigo, G., Barres De Almeida, U., et al. 2018, arXiv e-prints, arXiv:1805.08505  
 Giommi, P., Brandt, C. H., Barres de Almeida, U., et al. 2019, *A&A*, 631, A116  
 Giommi, P., Glauch, T., Padovani, P., et al. 2020a, arXiv e-prints, arXiv:2001.09355  
 Giommi, P., Glauch, T., & Resconi, E. 2020b, *The Astronomer’s Telegram*, 13394, 1  
 Harrison, F. A., Craig, W. W., Christensen, F. E., et al. 2013, *ApJ*, 770, 103  
 IceCube Collaboration. 2014, *Phys. Rev. Lett.*, 113, 101101  
 IceCube Collaboration. 2017a, arXiv e-prints, arXiv:1710.01179  
 IceCube Collaboration. 2017b, arXiv e-prints, arXiv:1710.01191  
 IceCube Collaboration. 2018, *Science*, 361, 147  
 IceCube Collaboration et al. 2018, *Science*, 361, eaat1378  
 Kalfountzou, E., Jarvis, M. J., Bonfield, D. G., & Hardcastle, M. J. 2012, *MNRAS*, 427, 2401  
 Keivani, A., Murase, K., Petropoulou, M., et al. 2018, *ApJ*, 864, 84  
 Krauss, F., Gregoire, T., Fox, D. B., Kennea, J., & Evans, P. 2020, *The Astronomer’s Telegram*, 13395, 1  
 Kronmueller, M. & Glauch, T. 2020, *PoS, ICRC2019*, 937  
 Liu, R.-Y., Wang, K., Xue, R., et al. 2019, *Phys. Rev. D*, 99, 063008  
 Lucarelli, F., Tavani, M., Piano, G., et al. 2019, *ApJ*, 870, 136  
 Murase, K., Oikonomou, F., & Petropoulou, M. 2018, *ApJ*, 865, 124  
 Oikonomou, F., Murase, K., Padovani, P., Resconi, E., & Mészáros, P. 2019, *MNRAS*, 489, 4347  
 Padovani, P. & Giommi, P. 1995, *ApJ*, 444, 567  
 Padovani, P., Giommi, P., Resconi, E., et al. 2018, *MNRAS*, 480, 192  
 Padovani, P., Oikonomou, F., Petropoulou, M., Giommi, P., & Resconi, E. 2019, *MNRAS*, 484, L104  
 Padovani, P. & Resconi, E. 2014, *MNRAS*, 443, 474  
 Padovani, P., Resconi, E., Giommi, P., Arsioli, B., & Chang, Y. L. 2016, *MNRAS*, 457, 3582  
 Paiano, S., Falomo, R., Padovani, P., et al. 2020, *MNRAS*, 495, L108  
 Paiano, S., Falomo, R., Treves, A., & Scarpa, R. 2018, *ApJ*, 854, L32  
 Petropoulou, M., Murase, K., Santander, M., et al. 2020, *ApJ*, 891, 115  
 Pizzuto, A. 2020, *GCN*, 26704, 1  
 Pogge, R. W., Atwood, B., Brewer, D. F., et al. 2010, *Proc. SPIE*, 7735, 77350A  
 Resconi, E., Coenders, S., Padovani, P., Giommi, P., & Caccianiga, L. 2017, *MNRAS*, 468, 597  
 Roming, P. W. A., Kennedy, T. E., Mason, K. O., et al. 2005, *Space Sci. Rev.*, 120, 95  
 Sbarrato, T., Ghisellini, G., Maraschi, L., & Colpi, M. 2012, *MNRAS*, 421, 1764  
 Schneider, A. 2020, *PoS, ICRC2019*, 1004  
 Stein, R. 2020, *GCN*, 26655, 1  
 Stettner, J. 2020, *PoS, ICRC2019*, 1017  
 Xue, R., Liu, R.-Y., Petropoulou, M., et al. 2019, *ApJ*, 886, 23  
 Zhang, B. T., Petropoulou, M., Murase, K., & Oikonomou, F. 2020, *ApJ*, 889, 118